Original Research

LKB1-AMPK modulates nutrient-induced changes in the mode of division of intestinal epithelial crypt cells in mice

Katherine Blackmore, Weinan Zhou and Megan J Dailey

Department of Animal Sciences, University of Illinois at Urbana-Champaign, Urbana, IL 61801, USA
Corresponding author: Megan J Dailey. Email: mdailey5@illinois.edu

Impact statement

The underlying cell biology of changes in the polarity of mitotic spindles and its relevance to tissue growth is a new concept and, thus, these data provide novel findings to begin to explain how this process contributes to the regeneration and growth of tissues. We find that short-term changes in food intake *in vivo* or glucose availability *in vitro* dictate the mode of division of crypt cells. In addition, we find that LKB1-AMPK signaling modulates the glucose-induced changes in the mode of division *in vitro*. Identifying mechanisms involved in the mode of division may provide new targets to control tissue growth.

Abstract

Nutrient availability influences intestinal epithelial stem cell proliferation and tissue growth. Increases in food result in a greater number of epithelial cells, villi height and crypt depth. We investigated whether this nutrient-driven expansion of the tissue is the result of a change in the mode of intestinal epithelial stem cell division and if LKB1-AMPK signaling plays a role. We utilized *in vivo* and *in vitro* experiments to test this hypothesis. C57BL/6J mice were separated into four groups and fed varying amounts of chow for 18 h: (1) ad libitum, (2) 50% of their average daily intake (3) fasted or (4) fasted for 12 h and refed. Mice were sacrificed, intestinal sections excised and immunohistochemically processed to determine the mitotic spindle orientation. Epithelial organoids *in vitro* were treated with no (0 mM), low (5 mM) or high (20 mM) amounts of glucose with or without an activator (Metformin) or inhibitor (Compound C) of LKB1-AMPK signaling. Cells were then processed to determine the mode of stem cell division. Fasted mice show a greater % of asymmetrically dividing cells compared with the other feeding groups. Organoids incubated with 0 mM glucose resulted in a greater % of asymmetrically dividing cells compared with the low or high-glucose conditions. In addition, LKB1-AMPK activation attenuated the % of symmetric division normally seen in high-glucose conditions. In contrast, LKB1-AMPK inhibition attenuated the % of asymmetric division normally seen in no glucose conditions. These data suggest that nutrient availability dictates the mode of division and that LKB1-AMPK mediates this nutrient-driven effect on intestinal epithelial stem cell proliferation.

Keywords: Intestine, stem cell, mode of division, LKB1-AMPK, nutrient, growth

***Experimental Biology and Medicine* 2017; 242: 1490–1498. DOI: 10.1177/1535370217724427**

Introduction

The availability of nutrients can dictate the size of many tissues. Somatic stem cells sense the level of nutrients and increase or decrease the rate of proliferation to grow or retract tissue size, respectively.[1,2] Stem cells have also been found to change their mode of division, from asymmetric to symmetric, in order to increase the number of cells during development, after injury or in abnormal tissue growth.[3,4] Whether changing the mode of stem cell division is utilized as a means of normal nutrient-induced mammalian tissue growth is unknown. The ability to switch cell division modes would allow stem cells to respond to the environment and change tissue size, but an ''on'' and ''off'' switch mechanism would be needed in order to maintain a balance in proliferation and prevent aberrant growth. Thus, identifying the mechanisms underlying nutrient-induced stem cell proliferation would provide new targets for pharmacological manipulation to control tissue growth.

Changes in the mode of cell division require alignment of the mitotic spindle in an orientation parallel to the apical-basal axis and polarized localization of cell fate determinants to the apical or basal poles of the cell. This allows for two molecularly distinct cells to be produced and for the two cells to develop in different environments (one towards the apical border and the other towards the basal; see Figure 1). The trigger for apical-basal protein localization and spindle orientation is unknown, but likely involves a metabolic cue. The best characterized of these is initiated by the activity of adenylate kinases that buffer declining ATP production by converting two ADPs to one ATP and one AMP. The accumulation of AMP activates AMP-activated protein kinase (AMPK). This activation is dependent on the

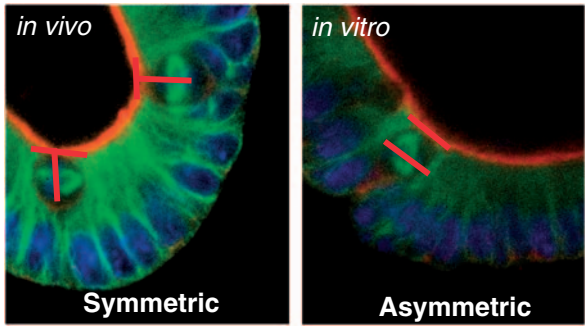

Figure 1 Representative photomicrograph of symmetric (left) and asymmetric (right) divisions. Green = microtubules (α-tubulin); Blue = nucleus (Dapi); Red = apical border. Note that the chromosome alignment is in an orientation perpendicular to the apical border in symmetric division and parallel in asymmetric. Whereas, the spindle poles are parallel in symmetric division and perpendicular in asymmetric

tumor suppressor protein LKB1 and leads to phosphorylation of several targets to improve the energy status in cells.[5] The role of the LKB1-AMPK pathway (LKB1-AMPK) is well known in metabolism and growth[6] and mutations of the LKB1 (*aka*. STK11) gene lead to Peutz-Jeghers syndrome in humans, characterized by the development of benign polyps and an increased risk of developing cancer.[7] In non-mammalian species, LKB1, or the homologous Par-4, is known more widely as a PAR protein involved in directing the partitioning of molecules during asymmetric division.[8,9] Therefore, LKB1 is a likely candidate for linking metabolism with changes in polarity during cell division. Moreover, AMPK has been shown to directly interact with the microtubule-based spindle.[10] Thus, we propose that activation of the LKB1-AMPK pathway that occurs under low nutrient availability results in asymmetric division and the maintenance of tissue size. Inhibition of this pathway under high nutrient availability would result in greater symmetric division and an expansion of the stem cell pool, resulting in growth of the tissue once asymmetric division resumes.

A unique model of nutrient-induced stem cell proliferation and tissue growth is provided by the intestinal epithelium. Maintenance of this tissue is driven by continuous proliferation of intestinal epithelial stem cells (IESCs) localized near the base of the crypts and nutrient availability is known to affect tissue size.[11,12] *In vivo*, an increase in food intake or luminal nutrients results in a greater number of epithelial cells, villi height and crypt depth (methods include: intestinal transposition,[13] hyperphagic animal models (diet-induced obesity,[14] lactation,[15] cold exposure[16,17]), whereas, decreases in food intake or luminal nutrients does the opposite(methods include: fasts,[18] surgical bypass,[19,20] hibernation[22,22]). *In vitro*, varying the levels of specific nutrients or growth factors known to be indirectly related to nutrient abundance (*i.e.* insulin and insulin-like growth factor 1), correlates with the level of proliferation and intestinal epithelial organoid growth.[14,23] Thus, we used an *in vivo* and *in vitro* approach to test whether the level of nutrients dictates the mode of division in intestinal epithelial tissue. Mice were fed varying amounts of a rodent chow diet and were separated into four groups; (1) Ad libitum fed (Ad lib) (2) Fed 50% of the average daily intake (50% fed) (3) Fasted or (4) Fasted for 12 h and then refed (Fast-Refed). All mice were terminated and small intestinal tissue samples were collected and processed to visualize the orientation of division. *In vitro* analyses were performed on epithelial organoids treated with varying amounts of glucose and immunohistochemically processed to visualize the mitotic spindle orientation. We further tested whether LKB1-AMPK signaling mediates the nutrient-induced switch *in vitro* by activating or inhibiting this pathway using Metformin or Compound C, respectively, in no or high-glucose conditions.

Methods

In vivo methods

Animals. Male C57BL/6J mice (Jackson Laboratories, $n = 32$ at 2.5 months of age) were housed individually in modified single shoe box cages with a raised platform and lined with brown kraft paper for collection of food spillage and feces, which allows for a more accurate measurement of food intake. Mice acclimated for one week with ad libitum access to standard rodent chow diet (Teklad 22/5 Rodent Diet, Teklad Diets, Madison, WI) and tap water and maintained on a 12:12 light:dark cycle (lights on at 1000 h). Mice were weighed daily at 0900 h under a red safelight (Adorama, New York, NY). Room temperature was maintained at 21°C ± 1 with 60% relative humidity. All procedures were approved by the Institutional Animal Care and Use Committee at the University of Illinois Urbana-Champaign.

Following the one week acclimation, food intake was measured each day for four days and an average food intake for each animal was calculated. The average food intake (13.6 ± 0.5 kcal) and body weight (26.3 ± 0.3 g) were used to equally divide the animals into four feeding conditions; (1) Ad libitum fed (Ad lib) (2) Fed 50% of the average daily intake (50% fed) (3) Fasted or (4) Fasted for 12 h and then refed for 6 h (Fast-Refed). Even though mice fed Ad lib have the highest available nutrients, these mice might be in a homeostatic state of proliferation because they have maintained this level of intake for multiple days (during acclimation and the four days of daily intake measurements). Thus, we have included the Fast-Refed group in order to ensure that we capture ''growth'' of the epithelium. At 1600 h, food was taken away from the Fasted and Fast-Refed group, while the Ad lib group was given fresh food in excess of what the mice would normally eat. The 50% fed group was also given fresh food but only 50% of their average daily consumption. After 18 h in each feeding condition (at 1000 h), the mice were killed by decapitation under isoflurane anesthesia (Henry Schein Animal Health, Dublin, OH). An abdominal incision was then made and the intestine was exposed. We collected tissue from the duodenum, jejunum and ileum. To ensure that we are collecting similar segments of the intestine for analysis between animals, we measure from the pyloric sphincter, throw away the first cm and then collect a 2 cm sample to be processed for the

mitotic spindle orientation and two additional 5 mm segments to be processed for other measurements. We then measure from the cecum, throw away the first 1 cm and then collect a 2 cm sample to be processed for the mitotic spindle orientation and two additional 5 mm segments of the ileum. From the remaining jejunal segment, we measure from the middle and collect a 2 cm sample and additional 5 mm segments to be processed similarly to the duodenal and ileal segments.

Tissue fixation and sectioning. Each of the 2 cm intestinal segments were flushed with cold 1× phosphate-buffered saline (PBS) and then filled with 15 μM Taxol (S1150, Selleckchem, Boston, MA) diluted in 4% EM grade paraformaldehyde (PFA; Ted Pella, Redding, CA). Taxol was diluted from 10 mM to a working concentration of 15 μM in 1× PBS. The filled intestine was then placed into 3 mL of Taxol/PFA solution. Following a 6 h fixation in Taxol/PFA at RT, the tissue was immersed in 30% sucrose diluted in 1× PBS overnight at 4°C. Tissue was then embedded using Tissue-Tek O.C.T medium (25608-930, 22 VWR, Radnor PA) and sections were cut on a cryostat at 8 μm thickness and mounted onto charged glass microscope slides. Slides were left to dry overnight and then stored in slide boxes at RT before immunohistochemical processing.

Immunohistochemical processing for mitotic spindle orientation. Sections were washed with 1× PBS and then incubated in 0.5% Triton X-100 (Triton-X, Sigma-Aldrich) diluted in 1× PBS (Lonza, Walkersville, MD) for 5 min at RT. The slides were then marked along the edges with a hydrophobic marker (ImmEdge; Vector Laboratories, Burlingame, CA) to allow for on-slide processing. All solutions applied directly to slides used a volume of 400 uL per slide. Slides were incubated in blocking solution (0.3% Triton-X, Sigma-Aldrich, St. Louis, MO and 1% Bovine Serum Albumin, diluted in 1× PBS) for 20 min at RT followed by an overnight incubation at 4°C in rabbit monoclonal anti-α tubulin (DM1A) Alexa Fluor 488 conjugated antibody (Ab195887, Abcam, San Francisco, CA) at a 1:100 concentration diluted in the blocking solution. After rinsing in 1× PBS, sections were incubated in phalloidin AlexaFluor568 (A12380,ThermoFisher Scientific, Waltham MA) at 165 nM and 1 μg/ml DAPI (D1306, ThermoFisher Scientific, Waltham MA) diluted in 1× PBS for 15 min at RT. Slides were coverslipped with Permount mounting media (Fisher Scientific, Fair Lawn, NJ). Slides were stored short-term at RT and long-term at 4°C in light-proof boxes. Images of the sections were captured by digital camera attached to a Zeiss LSM700 Confocal Imager (Carl Zeiss MicroImaging, Inc., Thornwook, NY).

Calculation of spindle orientation. Several cell inclusion criteria were set prior to analysis. (1) Dividing cells had be clearly adjacent to, and not overlapping with, other cells. (2) Dividing cells must be localized below the +4 position to exclude transit amplifying cells as described previously.[24,25] (3) The crypt had to have a clear basal border, apical border and intercrypt lumen. (4) Tissue sections had to have clearly defined crypts adjacent to villi. (5) Cells had to have two defined spindle poles and spindle poles had to be in the same image plane. To determine the mode of division, the angle between the spindle poles and apical border was calculated using the ImageJ angle tool. As described previously,[3,26] an angle less than 30° was considered a symmetric division and an angle over 30° indicated asymmetric division when in a single image plane. All dividing cells per 8 μm section with a total of 48 μm total per duodenum, jejunum and ileum were analyzed per mouse. Results from the duodenum, jejunum and ileum are presented separately and pooled and presented as the whole organ.

Immunohistochemical processing for Ki67. Mounted tissue sections were heated for 30 min at 67°C. Sections were then washed in 1× PB and antigen retrieval was performed by immersing slides in Sodium Citrate Buffer (Sodium Citrate Hydrochloride, Fisher Scientific and Tween 20, Sigma-Aldrich, Germany, pH 6.0) for 20 min in a water bath at 95°C. Slides were allowed to cool for 30 min at RT and washed in PB. Tissue was then incubated in a blocking solution containing 0.3% Triton-X (Sigma-Aldrich, St. Louis, MO) and 3% Normal Donkey Serum (Jackson Immuno Research, West Grove, PA) diluted in 1×PB for 20 min at RT. After blocking, tissue was incubated overnight at 4°C in sheep monoclonal anti-Ki67 antibody (Santa Cruz Biotech, Dallas TX) at a 1:100 concentration diluted in the blocking solution. Tissue was then rinsed in 1× PB prior to incubation in a donkey anti-sheep biotinylated secondary antibody (Ab6899, Abcam, San Francisco, CA) at a 1:500 concentration diluted in 1× PB for 2 h at RT. After washing in 1× PB, the tissue sections were then incubated in an avidin–biotin complex (Vectastain Elite reagents, Vector Labs, Burlingame, CA) for 1 h at RT. Tissue was washed in 1× PB and then incubated in diaminobenzidine (SK-4100, Vector Laboratories, Burlingame, CA) for 10 min at RT for visualization. Sections were washed in 1× PB, left to dry overnight, then dehydrated in a series of graded ethanols and cleared in xylenes. Slides were coverslipped with Permount mounting media (Fisher Scientific, Fair Lawn, NJ) and stored at RT.

Quantification of proliferating intestinal stem cells. Intestinal tissue sections were visualized and quantified using the NanoZoomer Digital Pathology System (Hamamatsu, Hamamatsu City, Japan) and NDP View 2 software using a 40× objective; 5–10 crypts per 8 μm intestinal cross section was analyzed with a total of 48 μm from each segment of the intestine (duodenum, jejunum, ileum) per mouse. Inclusion criteria included that crypt morphology had to have distinct apical and basal borders and labeled cells must be localized below the +4 position to exclude transit amplifying cells, as previously described.[24,25] Quantification of proliferation was performed in two different ways; (1) number of positive Ki67 cells and (2) ratio of positive Ki67 to total number of cells in the proliferative zone. Furthermore, these data were analyzed both as whole organ (duodenal, jejunal and ileum

data combined) as well as by individual segments to detect differences from the proximal to distal axis.

In vitro methods

Isolation of small intestinal crypts and small intestinal crypt culture. Male C57BL/6J mice (Jackson Laboratories) at 2.5 months of age were sacrificed under isoflurane anesthesia and the intestine was exposed. Approximately 2 cm of each intestinal segment was excised, opened longitudinally and flushed with ice-cold PBS. Crypts were isolated as previously described.[27] Villi were scraped off using a coverslip and the tissue was washed with ice-cold PBS in a 50 mL conical tube. In a sterile cell culture hood, intestinal fragments were cut into 1 mm x × 1 mm squares and washed by gentle trituration in 30 mL of ice-cold 1× PBS. Supernatant was discarded and the procedure was repeated five to eight times. Fragments were incubated in 2 mM Ethylenediaminetetraacetic acid (Sigma Aldrich, Germany) diluted in 1× PBS at 4°C for 30 min with gentle rocking. The supernatant was removed and fragments were washed with 20 mL of ice cold 1× PBS. This was considered fraction 1. Fraction 1 was discarded and fragments were resuspended in 10 mL of 1× PBS. After gentle trituration fragments were allowed to settle and the supernatant (fraction 2) was removed and put in a 50 mL conical tube. This was repeated two more times, each time adding the supernatant to the tube containing fraction 2. These are considered fractions 3 and 4. Crypt fractions were passed through a 70 μm cell strainer and spun down at 300 × *g*, 4C for 5 min. The pellet was resuspended in 10 mL of ice cold advanced DMEM/F12 (11320082, Gibco, Elmhurst, IL) supplemented with 2 mM GlutaMax (35050061, Gibco, Elmhurst, IL), 10 mM HEPES (15630080, Gibco, Elmhurst IL), and 100 U/mL penicillin/100 μg/mL streptomycin (15140148, Gibco, Elmhurst, IL). Crypt fractions were spun at 200 × *g*, 4C for 5 min to separate single cells. Crypts were counted using tryphan blue exclusion and an inverted light microscope. Crypts were then spun down and resuspended in Corning® Matrigel® Growth Factor Reduced (GFR) Basement Membrane Matrix (356231, Corning, Corning, NY) at 1000 crypts/50 μl. Fifty microliters of resuspended Matrigel™ was added to the center of a pre-warmed Millicell® EZ slide (1.7 cm^2 growing area per well) (EMD Millipore, Kankakee, IL). The plate was incubated in a CO_2 incubator (5% CO2, 37°C) for 10 min to allow the MatrigelTM to solidify and 500 μl of complete culture media (Basal culture medium with N2 supplement (1×), B27 supplement (1×), and 1 mM N-acetylcysteine, 50 ng/mL EGF, 100 ng/mL Noggin, 1 mg/mL R-spondin.). Primary crypt cultures were kept at 5% CO2, 37°C.

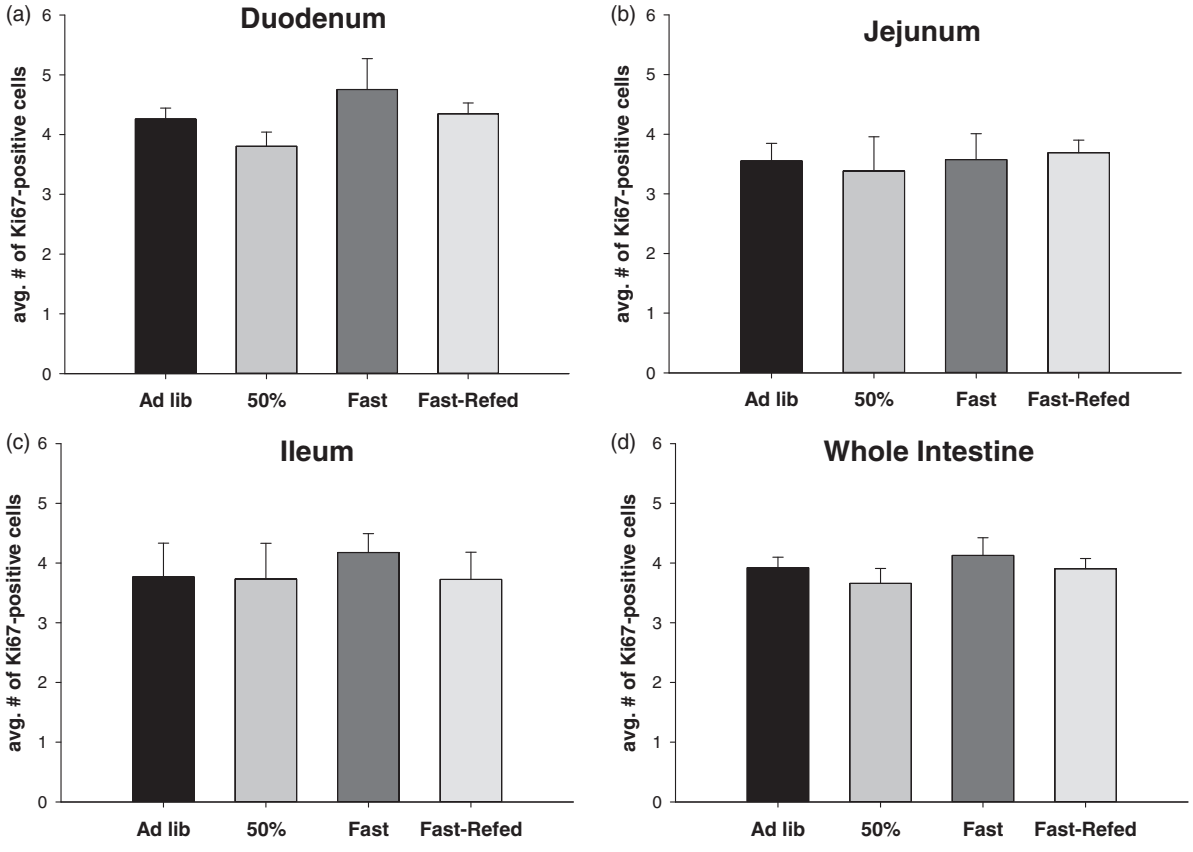

Figure 2 Food intake does not dictate the number of proliferating cells in the crypt base. Average number of Ki67-positive cell number in the crypt base of mice fed ad libitum (Ad lib), fed 50% of their normal daily intake (50% fed), fasted (Fasted), and fasted for 12 h and then refed (Fast-Refed) in the duodenum (a), jejunum (b), ileum (c) and combined as the whole intestine (d). $n = 8$ mice per group, 5–10 crypts per 5 μm intestinal cross section was analyzed with a total of 30 μm from each segment of the intestine (duodenum, jejunum, ileum) per mouse. Values are mean ± SEM. Data were analyzed using a one-way ANOVA. $P < 0.05$

In vitro *experimental design.* Following primary culture, crypts were allowed to grow for four days into epithelial organoids. At 0800 h on day 5, cultures were changed to glucose-free media (Basal culture medium with N2 supplement (1×), B27 supplement (1×), and 1 mM N-acetylcysteine, 50 ng/mL EGF, 100 ng/mL Noggin, 1 mg/mL R-spondin) and incubated at 37°C at 5% CO2 for 4 h. Organoid cultures were then supplied with glucose at one of three concentrations, 0 mM, 5 mM or 20 mM and incubated for 5 h. The glucose concentrations were chosen based on hepatic portal vein or systemic levels of glucose after or between meals in mice.[28,29] After glucose incubation, the organoid cultures were fixed, immunohistochemically processed and visualized as described for the *in vivo* mitotic spindle orientation experiments.

Activation or inhibition of LKB1-AMPK. Isolated crypts were allowed to grow for four days into epithelial organoids. At 0800 h on day 5, crypts were changed to glucose-free media and incubated at 37°C at 5% CO_2 for 4 h. Organoids were then supplied with 0 mM or 20 mM glucose and either 1 mM Metformin HCL (Ab120847, Abcam, San Francisco, CA), 1 mM Compound C (Ab120843, Abcam, San Francisco, CA) or a vehicle control (ddH2O for Metformin and 10% DMSO in PBS for Compound C). Following a 5 h incubation, organoids were fixed and immunohistochemically processed for visualization of the mitotic spindle orientation as described above.

Statistical analysis. Values are expressed as the mean ± SEM. Mode of division data were analyzed based on the % of asymmetrically dividing cells in each group. Data from the *in vivo* and *in vitro* glucose concentration experiments were analyzed using a one-way ANOVA (feeding conditions or glucose concentration as independent measures). A two-way ANOVA was used to analyze the effect of LKB1-AMPK signaling on the mode of division (2 × 2; glucose concentration x drug treatment). Tukey–Kramer *post hoc* analysis was utilized, when appropriate, and differences among groups were considered statistically significant if $P < 0.05$.

Results

Number of proliferating cells

There was no significant difference in Ki67-positive cell number in the crypt zone across the feeding conditions when the individual intestinal segments were analyzed (Figure 2(a) to (c)) or when the segments were pooled and

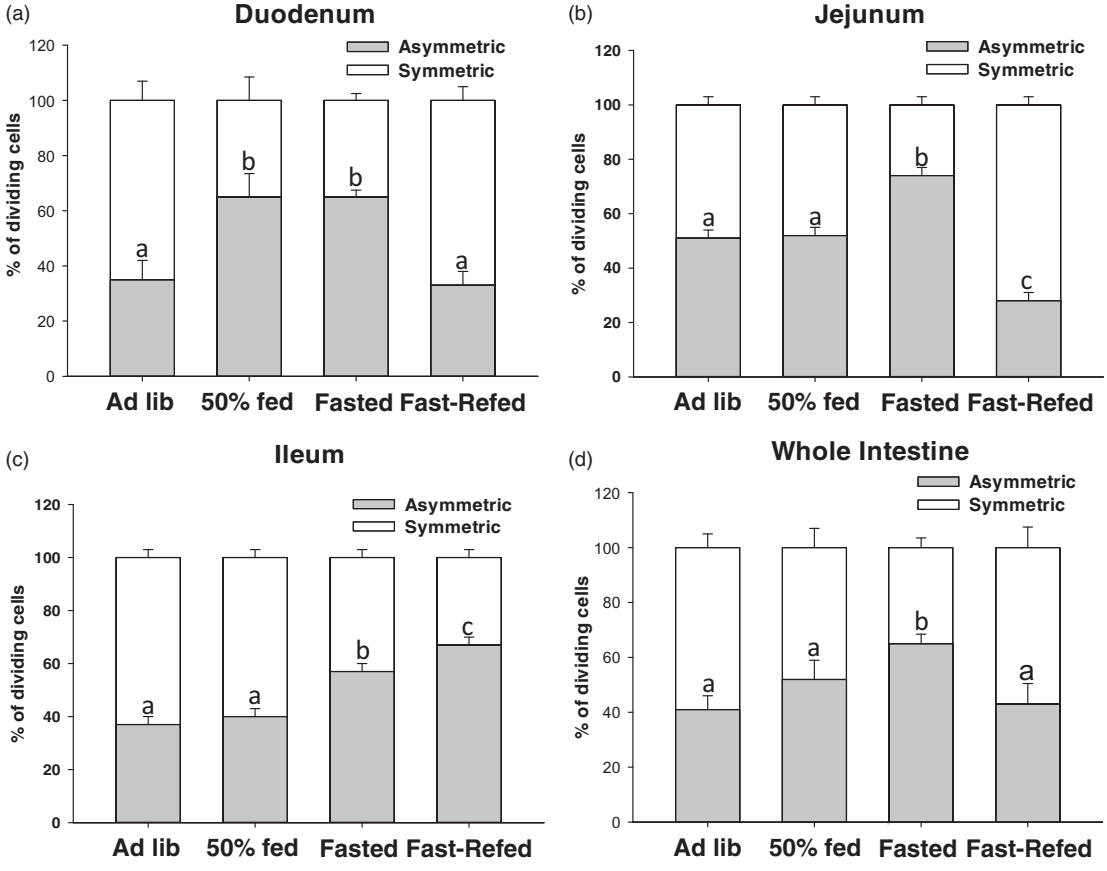

Figure 3 Food intake dictates the mode of division of proliferating cells in the crypt base. % of dividing cells that were asymmetrically or symmetrically dividing in mice fed ad libitum (Ad lib), fed 50% of their normal daily intake (50% fed), fasted (Fasted), and fasted for 12 h and then refed (Fast-Refed) in the duodenum (a), jejunum (b), ileum (c) and combined as the whole intestine (d). $n = 8$ mice per group, all dividing cells per 5 μm section was analyzed with a total of 30 μm from each segment of the intestine (duodenum, jejunum, ileum) per mouse. Values are mean ± SEM. % of asymmetric division data were analyzed using a one-way ANOVA. Tukey–Kramer *post hoc* analysis was performed. Means with different letters are significantly different. Means with different letters indicate significantly different, $P < 0.05$

analyzed as a whole organ (Figure 2(d)). There was also no difference in the ratio of Ki67-positive cells to total number of cells in the proliferative zone (data not shown).

In vivo mode of division

In the duodenum, the Ad lib and Fasted-Refed groups had a significantly lower % of asymmetrically dividing cells compared with the 50% fed and the Fasted groups (Figure 3(a); $P < 0.05$). In the jejunum, the % of asymmetrically dividing cells was significantly higher in the Fasted group compared with all other groups (Figure 3(b); $P < 0.05$), whereas the Fasted-Refed group had a significantly lower % of asymmetric division compared with all other groups in the jejunum (Figure 3(b); $P < 0.05$). There was not a difference between the Ad lib and 50% fed groups in the jejunum (Figure 3(b)). In the ileum, the % of asymmetrically dividing cells was the highest in the Fasted-Refed group compared with all other groups (Figure 3(c); $P < 0.05$). The Fasted group had a significantly higher % of asymmetric division compared with the Ad lib and 50% fed, but a significantly lower % than the Fasted-Refed group (Figure 3(c); $P < 0.05$). There was no difference between the Ad lib and 50% fed groups in the ileum. When analyzed as a whole organ, there was a greater % of asymmetric division in the Fasted group compared with the other groups (Figure 3(d); $P < 0.05$). No significant difference in the % of asymmetric division was found between the Ad lib, 50% fed or Fast-Refed (Figure 3(d); $P < 0.05$).

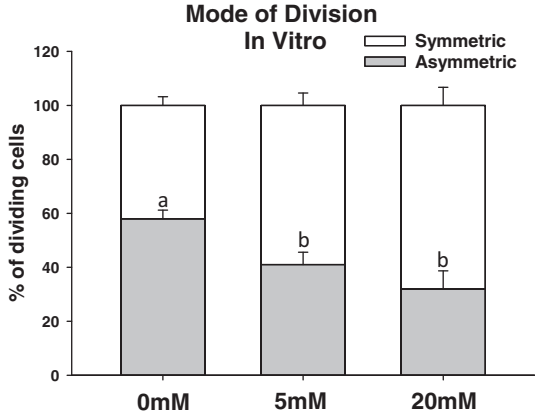

Figure 4 Glucose availability *in vitro* dictates the mode of division of proliferating crypt cells. Intestinal epithelial ids from mice were glucose deprived for 4 h and then incubated with 0 mM, 5 mM or 20 mM glucose for 5 h. Organoids were then immunohistochemically processed in order to determine the mitotic spindle orientation. All dividing crypt base cells per well (run in triplicate for each mouse) were analyzed. Values are mean ± SEM. % of asymmetric division data were analyzed using a one-way ANOVA. Tukey–Kramer *post hoc* analysis was performed. Means with different letters are significantly different. Means with different letters indicate significantly different, $P < 0.05$

In vitro mode of division

There was a greater % of asymmetric division in the 0 mM glucose condition compared with the 5 mM and 20 mM glucose conditions (Figure 4; $P < 0.05$). No significant difference in the % asymmetric division was found between the 5 mM and 20 mM glucose conditions (Figure 4).

Activation and inhibition of LKB1-AMPK

There was a significant decrease in the % of asymmetrically dividing cells in the high (20 mM) glucose condition compared with the no glucose condition (Figure 5(a); $P < 0.05$). Metformin, or the activation of AMPK signaling, induced greater asymmetric division even in high (20 mM) glucose conditions (Figure 5(a); $P < 0.05$). There was a greater % of asymmetrically diving cells in the 0 mM glucose without Compound C compared with the other groups (Figure 5(b);

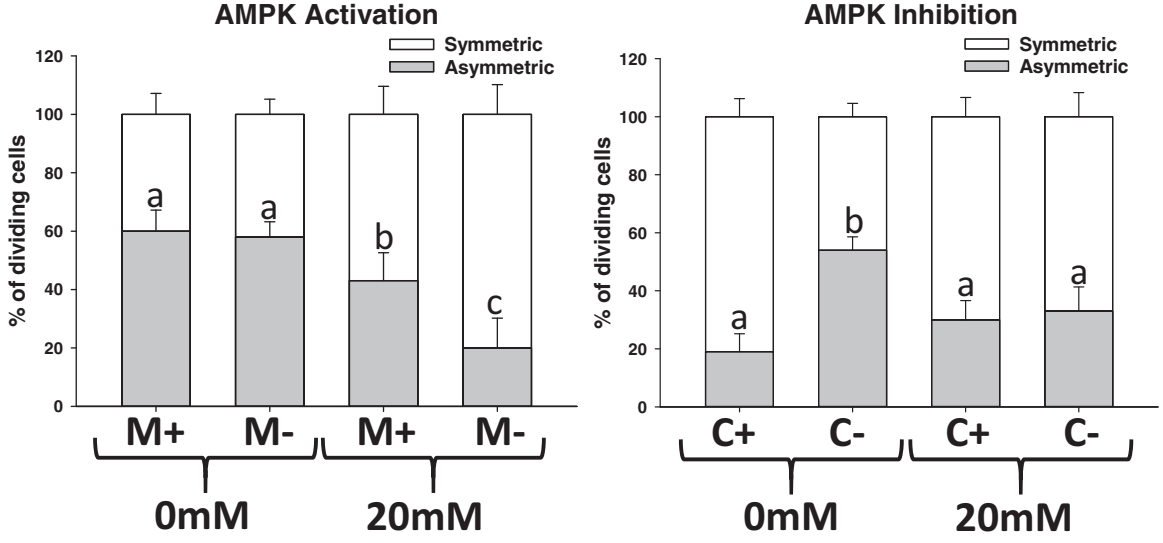

Figure 5 AMPK modulates the glucose-driven effect on the mode of proliferation *in vitro*. (a) Activation of AMPK using Metformin (M) induces greater asymmetric division in a high-glucose (20 mM) condition. (b) Inhibition of AMPK using Compound C (c) blocks the switch to asymmetric division normally seen in no glucose conditions. Epithelial organoids from mice were glucose deprived for 4 h and then incubated with 0 mM or 20 mM in the presence or absence of M or C. All dividing crypt base cells per well (run in triplicate for each mouse) were analyzed. Values are mean ± SEM. % of asymmetric division data were analyzed using a one-way ANOVA. Tukey–Kramer post hoc analysis was performed. Means with different letters indicate significantly different, $P < 0.05$

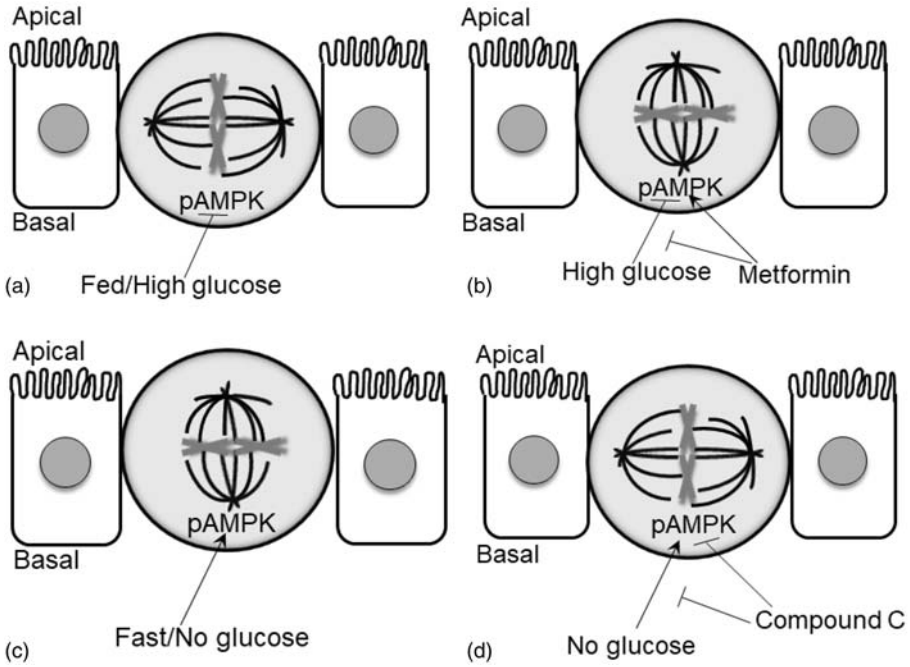

Figure 6 Graphical representation summarizing the nutrient-induced effect on the mode of proliferation. (a) Fed mice *in vivo* or high glucose *in vitro* inhibits the phosphorylation of AMPK (pAMPK) and results in vertical cleavage and symmetric division. (b) Metformin, an activator of AMPK, blocks the high glucose-induced effect *in vitro* and results in horizontal cleavage and asymmetric division. (c) Fasted mice *in vivo* or no glucose *in vitro* stimulates the phosphorylation of AMPK and results in horizontal cleavage and asymmetric division. (d) Compound C, an inhibitor of pAMPK, blocks the no glucose-induced effect *in vitro* and results in vertical cleavage and symmetric division

$P < 0.05$). Compound C, or the inhibition of LKB1-AMPK, increased the % of symmetrically dividing cells even under a no glucose condition (Figure 5(b); $P < 0.05$). There was no effect of Compound C under the high (20 mM) glucose condition (Figure 5).

Discussion

The aim of these experiments was to investigate if nutrient availability alters the mode of division in IESCs and whether LKB1-AMPK plays a role in this nutrient-driven response in proliferation. The lead findings were: (1) the amount of food intake did not affect the number of proliferating cells in the crypt base, (2) the amount of food intake changes the mode of proliferation *in vivo*, (3) glucose availability changes the mode of proliferation *in vitro*, (4) LKB1-AMPK activation attenuated the % of symmetric division normally seen in high-glucose conditions and (5) LKB1-AMPK inhibition attenuated the % of asymmetric division normally seen in no glucose conditions (summarized in Figure 6).

It is not clear if there is an actual switch in the mode of division in a single stem cell, or if the nutrient-induced division pattern is represented by a population of stem cells where a subset divides asymmetrically and the other symmetrically. Although AMPK has been shown to directly modify the microtubules and spindle orientation in a single cell,[10] it is possible that a subset of stem cells may always divide asymmetrically while another divides symmetrically. Nutrient availability may then differentially affect each population. Even if this is the case, LKB1-AMPK appears to still be a mechanism by which high or low nutrient levels induces proliferation in only the symmetric or asymmetric population, respectively.

Symmetric division can result in duplication of the IESC (self-renewal) or loss of the IESC due to production of two daughter cells that differentiate (non-stem cell fate). Although data support the notion that high nutrient availability induces symmetric self-renewal in order to increase the number of stem cells and grow the tissue once asymmetric division begins again,[30] it is possible that there is also a switch between the two types of symmetric division patterns under nutritional variability. Lineage-tracing experiments can reveal whether the stem cells duplicate themselves or extinguish themselves by producing two daughter cells.[31] When lineage-tracing was performed in *Drosophila*, the two types of symmetric division patterns are followed at equal rates and, thus, maintained the epithelium at a constant size.[30] When high nutrient intake is maintained in mice over several months using a diet-induced obese model, an increase in the stem cell pool is seen suggesting that the IESCs did indeed divide utilizing a symmetric self-renewal pattern.[14,23] Thus, we believe that the greater % of symmetric division that we see may also be represented by the IESC self-renewal pattern under acute changes in nutrients.

The glucose-dependent change in the mode of proliferation that we found *in vitro* mimics the many studies that find a correlation between the amount of luminal nutrients and crypt cell proliferation or growth of the epithelium *in vivo*.[13,14,17,23,32] That said, it is not clear if the glucose levels that we chose to use are representative of the levels

of glucose in the crypt microenvironment. Systemic levels of glucose in C57BL/6J mice, the strain utilized in the present study, vary greatly, but generally fall ~5 mM during acute fasts and as high as ~20 mM after meals.[29,33–35] These systemic values, though, may not be the same within the crypt microenvironment. The IESCs within the crypt are likely affected by the concentration of nutrients in the venules that would include ingested nutrients, systemic levels of nutrients supplied to the crypts by the superior mesenteric artery and cells underlying the crypt epithelium within the lamina propria. Thus, we do not know if the exact levels of glucose utilized reflect the *in vivo* crypt environment. We can only conclude that the crypt cells are able to respond to varying glucose levels by altering proliferation.

Conclusion

The ability of stem cells to divide asymmetrically or symmetrically allows for flexibility of a tissue to expand or retract in size based on cues in the stem cell niche. We show that nutrient availability is such a cue and that a metabolic protein-kinase network is able to mediate this effect. How the stem cells sense the level of nutrients to induce these changes, though, is still unknown. This may involve a direct effect of nutrients on membrane transporters or receptors (e.g. the differential affinity of glucose transporters for glucose) or, as has been suggested by others, an indirect mechanism that involves growth hormones whose levels correctly reflect nutrient abundance. Understanding the normal mechanisms underlying changes in the mode of stem cell proliferation may elucidate signaling that lead to abnormal tissue growth and provide a way to be able to reverse the negative proliferative effects.

Authors' contributions: Author contributions: KAB and MJD conception and design of research; KAB and WZ performed experiments; KAB and MJD analyzed data; KAB and MJD interpreted results of experiments; KAB prepared figures; KAB and MJD drafted manuscript; KAB, WZ and MJD edited and revised manuscript; KAB, WZ and MJD approved final version of manuscript.

ACKNOWLEDGEMENTS

We would like to thank Matthew Bertagne and Ashton Townsley for their immense contribution in tissue processing and quantification. This work was supported by USDA Hatch ILLU-538-926 (to MJ Dailey).

DECLARATION OF CONFLICTING INTERESTS

The author(s) declared no potential conflicts of interest with respect to the research, authorship, and/or publication of this article.

REFERENCES

1. Ochocki JD, Simon MC. Nutrient-sensing pathways and metabolic regulation in stem cells. *J Cell Biol* 2013;**203**:23–33
2. Puig O, Tjian R. Nutrient availability and growth: regulation of insulin signaling by dFOXO/FOXO1. *Cell Cycle* 2006;**5**:503–5
3. Quyn AJ, Appleton PL, Carey FA, Steele RJ, Barker N, Clevers H, Ridgway RA, Sanson OJ, Nathke IS. Spindle orientation bias in gut epithelial stem cell compartments is lost in precancerous tissue. *Cell Stem Cell* 2010;**6**:175–81
4. Morrison SJ, Kimble J. Asymmetric and symmetric stem-cell divisions in development and cancer. *Nature* 2006;**441**:1068–74
5. Kahn BB, Alquier T, Carling D, Hardie DG. AMP-activated protein kinase: ancient energy gauge provides clues to modern understanding of metabolism. *Cell Metab* 2005;**1**:15–25
6. Shackelford DB, Shaw RJ. The LKB1-AMPK pathway: metabolism and growth control in tumour suppression. *Nat Rev Cancer* 2009;**9**:563–75
7. Mehenni H, Gehrig C, Nezu J, Oku A, Shimane M, Rossier C, Guex N, Blouin JL, Scott HS, Antonarakis SE. Loss of LKB1 kinase activity in Peutz-Jeghers syndrome, and evidence for allelic and locus heterogeneity. *Am J Hum Genet* 1998;**63**:1641–50
8. Benkemoun L, Descoteaux C, Chartier NT, Pintard L, Labbe JC. PAR-4/LKB1 regulates DNA replication during asynchronous division of the early C. elegans embryo. *J Cell Biol* 2014;**205**:447–55
9. Bonaccorsi S, Mottier V, Giansanti MG, Bolkan BJ, Williams B, Goldberg ML, Gatti M. The Drosophila Lkb1 kinase is required for spindle formation and asymmetric neuroblast division. *Development* 2007;**134**:2183–93
10. Thaiparambil JT, Eggers CM, Marcus AI. AMPK regulates mitotic spindle orientation through phosphorylation of myosin regulatory light chain. *Mol Cell Biol* 2012;**32**:3203–17
11. van der Flier LG, Clevers H. Stem cells, self-renewal, and differentiation in the intestinal epithelium. *Ann Rev Physiol* 2009;**71**:241–60
12. Leblond CP, Stevens CE. The constant renewal of the intestinal epithelium in the albino rat. *Anatom Record* 1948;**100**:357–77
13. Altmann GG, Leblond CP. Factors influencing villus size in the small intestine of adult rats as revealed by transposition of intestinal segments. *Am J Anatomy* 1970;**127**:15–36
14. Mah AT, Van Landeghem L, Gavin HE, Magness ST, Lund PK. Impact of diet-induced obesity on intestinal stem cells: hyperproliferation but impaired intrinsic function that requires insulin/IGF1. *Endocrinology* 2014;**155**:3302–14
15. Crean GP, Rumsey RD. Hyperplasia of the gastric mucosa during pregnancy and lactation in the rat. *J Physiol* 1971;**215**:181–97
16. Toloza EM, Lam M, Diamond J. Nutrient extraction by cold-exposed mice: a test of digestive safety margins. *Am J Physiol* 1991;**261**(4 Pt 1): G608–20
17. Kaushik S, Kaur J. Effect of chronic cold stress on intestinal epithelial cell proliferation and inflammation in rats. *Stress* 2005;**8**:191–7
18. Ross GA, Mayhew TM. Effects of fasting on mucosal dimensions in the duodenum, jejunum and ileum of the rat. *J Anatomy* 1985;**142**:191–200
19. Gleeson MH, Cullen J, Dowling RH. Intestinal structure and function after small bowel by-pass in the rat. *Clin Sci* 1972;**43**:731–42
20. Robinson JW, Menge H, Schroeder P, Riecken EO, van Melle G. Structural and functional correlations in the atrophic mucosa of self-emptying blind loops of rat jejunum. *Eur J Clin Invest* 1980;**10**:393–9
21. Carey HV, Cooke HJ. Effect of hibernation and jejunal bypass on mucosal structure and function. *Am J Physiol* 1991;**261**(1 Pt 1): G37–44
22. Carey HV. Seasonal changes in mucosal structure and function in ground squirrel intestine. *Am J Physiol* 1990;**259**(2 Pt 2): R385–92
23. Beyaz S, Mana MD, Roper J, Kedrin D, Saadatpour A, Hong SJ, Bauer-Rowe KE, Xifaras ME, Akkad A, Arias E, Pinello L, Katz Y, Shinagare S, Abu-Remaileh M, Mihaylova MM, Lamming DW, Dogum R, Guo G, Bell GW, Selig M, Nielsen GP, Gupta N, Ferrone CR, Deshpande V, Yuan GC, Orkin SH, Sabatini DM, Yilmaz OH. High-fat diet enhances stemness and tumorigenicity of intestinal progenitors. *Nature* 2016;**531**:53–8
24. Barker N, van Oudenaarden A, Clevers H. Identifying the stem cell of the intestinal crypt: strategies and pitfalls. *Cell Stem Cell* 2012;**11**:452–60
25. Potten CS, Gandara R, Mahida YR, Loeffler M, Wright NA. The stem cells of small intestinal crypts: where are they? *Cell Prolif* 2009;**42**:731–50
26. Fleming ES, Zajac M, Moschenross DM, Montrose DC, Rosenberg DW, Cowan AE, Tirnauer JS. Planar spindle orientation and asymmetric cytokinesis in the mouse small intestine. *J Histochem Cytochem* 2007;**55**:1173–80

27. Sato T, Clevers H. Primary mouse small intestinal epithelial cell cultures. *Methods Mol Biol* 2013;**945**:319–28
28. Ayala JE, Samuel VT, Morton GJ, Obici S, Croniger CM, Shulman GI, Wasserman DH, McGuinness OP, NIH Mouse Metabolic Phenotyping Center Consortium. Standard operating procedures for describing and performing metabolic tests of glucose homeostasis in mice. *Dis Model Mech* 2010;**3**:525–34
29. Han BG, Hao CM, Tchekneva EE, Wang YY, Lee CA, Ebrahim B, Harris RC, Kern TS, Wasserman DH, Breyer MD, Qi Z. Markers of glycemic control in the mouse: comparisons of 6-h- and overnight-fasted blood glucoses to Hb A1c. *Am J Physiol Endocrinol Metab* 2008;**295**:E981–6
30. O'Brien LE, Soliman SS, Li X, Bilder D. Altered modes of stem cell division drive adaptive intestinal growth. *Cell* 2011;**147**:603–14
31. Barker N, van Es JH, Kuipers J, Kujala P, van den Born M, Cozijnsen M, Haegebarth A, Korving J, Begthel H, Peters PJ, Clevers H. Identification of stem cells in small intestine and colon by marker gene Lgr5. *Nature* 2007;**449**:1003–7
32. Cripps AW, Williams VJ. The effect of pregnancy and lactation on food intake, gastrointestinal anatomy and the absorptive capacity of the small intestine in the albino rat. *Br J Nutr* 1975;**33**:17–32
33. Savontaus E, Fagerholm V, Rahkonen O, Scheinin M. Reduced blood glucose levels, increased insulin levels and improved glucose tolerance in alpha2A-adrenoceptor knockout mice. *Eur J Pharmacol* 2008;**578**:359–64
34. Berglund ED, Li CY, Poffenberger G, Ayala JE, Fueger PT, Willis SE, Jewell MM, Powers AC, Wasserman DH. Glucose metabolism in vivo in four commonly used inbred mouse strains. *Diabetes* 2008;**57**:1790–9
35. Klueh U, Liu Z, Cho B, Ouyang T, Feldman B, Henning TP, Kaur M, Kreutzer D. Continuous glucose monitoring in normal mice and mice with prediabetes and diabetes. *Diab Technol Ther* 2006;**8**:402–12

(Received March 28, 2017, Accepted July 13, 2017)